mathematics

MDPI

Article

A Novel Coupled Memristive Izhikevich Neuron Model and Its Complex Dynamics

Fengling Jia [1], Peiyan He [2] and Lixin Yang [2,*]

[1] School of Mathematics, Chengdu Normal University, Chengdu 611130, China; cdjiafl@163.com
[2] College of Mathematics and Data Science, Shaanxi University of Science and Technology, Xi'an 710021, China; peiyhe@163.com
* Correspondence: yanglixin@sust.edu.cn

Abstract: This paper proposes a novel, five-dimensional memristor synapse-coupled Izhikevich neuron model under electromagnetic induction. Firstly, we analyze the global exponential stability of the presented system by constructing an appropriate Lyapunov function. Furthermore, the Hamilton energy functions of the model and its corresponding error system are derived by using Helmholtz's theorem. In addition, the influence of external current and system parameters on the dynamical behavior are investigated. The numerical simulation results indicate that the discharge pattern of excitatory and inhibitory neurons changes significantly when the amplitude and frequency of the external stimulus current are applied at different degrees. And the crucial dynamical behavior of the neuronal system is determined by the intensity of modulation of the induced current and the gain in the electromagnetic induction. Moreover, the amount of Hamilton energy released by the model could be evaluated during the conversion between the distinct dynamical behaviors.

Keywords: five-dimensional neuron model; Hamilton energy; dynamical behaviors

MSC: 34D06; 37M05

check for updates

Citation: Jia, F.; He, P.; Yang, L. A Novel Coupled Memristive Izhikevich Neuron Model and Its Complex Dynamics. *Mathematics* **2024**, *12*, 2244. https://doi.org/10.3390/math12142244

Academic Editor: Jonathan Blackledge

Received: 28 June 2024
Revised: 17 July 2024
Accepted: 18 July 2024
Published: 18 July 2024

Copyright: © 2024 by the authors. Licensee MDPI, Basel, Switzerland. This article is an open access article distributed under the terms and conditions of the Creative Commons Attribution (CC BY) license (https://creativecommons.org/licenses/by/4.0/).

1. Introduction

Neurons are the basic structure and function of the nervous system; they are the foundation of the brain. There are about 10^{11} neurons in the brain, which can perceive changes in the environment and complete the reception and transmission of information. And these neurons have some crucial properties, such as excitability, conductivity, and plasticity. Therefore, it is necessary to study the dynamical behavior of neurons. Many researchers tend to use mathematical models with parameters to describe neurons and use these models to study the complex nonlinear behavior of neurons [1]. With the further consideration and improvement of the neuron model by researchers, the Hodgkin–Huxley neuron, Fitzhugh–Nagumo neuron, Morris–Lecar neuron, Chay neuron, Hindmarsh–Rose neuron, Izhikevich neuron, Hopfield neural network, and TrueNorth chip models [2–10] were proposed successively, and these models have become major tools for computational neuroscience research.

In recent years, many works have concentrated on the discharge activity and rich nonlinear dynamics of single neurons and neuronal networks [11–13]. These studies provided an analytical mechanism for neurons to participate in information coding and energy metabolism during brain operation. Lakshmanan et al. [14] analyzed the stability, bifurcation, and chaos of the Hindmarsh–Rose neuron model with time delay, it was found that the neuron model can show different discharge behaviors by setting corresponding bifurcation parameters, and the enactment of synchronization criteria can make the system achieve global asymptotic stability. In [15], the authors took into account the method in which two FHN neuron circuits are coupled with a Josephson junction and realized the synchronization stability of the whole neural circuit by adjusting the parameters of the

Josephson junction in the coupling channel. And the investigation results revealed that the synchronization between the neural circuits is determined by the coupling method and also depends on the physical properties of the nonlinear oscillator in the coupling channel. In fact, the activation of magnetic field coupling is the result of the continuous release and propagation of intracellular and extracellular ions. Therefore, magnetic field coupling may play a crucial role in modulating collective behavior among neurons.

Importantly, the fluctuation in ion concentration inside and outside the cell membrane would cause changes in electromagnetic field distribution inside and outside the cell, resulting in electromagnetic induction. The influence of the electromagnetic effect should be considered in many investigations of neurons [16,17]. A memristor is a kind of circuit element with memory characteristics which is defined by magnetic flux and charge. A memristor can be used to simulate the synapses of biological neurons, and memristor synapses can be used to characterize this electromagnetic effect [18]. Xu et al. [19] established a bi-neuron Rulkov network with a memristive synapse and explored the multi-stability and phase synchronization of a neural network; it was also observed that the dynamical behaviors of the neural network depended on the setting of the synaptic coupling strength and initial value, and the neural network could produce rich discharge patterns under the influence of different conditions. Kafraj et al. [20] discussed the dynamical behaviors of neurons under electromagnetic induction and noise by virtue of the memristive Izhikevich neuron model. Their studies revealed that the neuron model showed complex discharge modes under different parameter conditions. Mondal et al. [21] established a single Izhikevich neuron under periodic signal stimulation; the chaotic resonance of the model could produce corresponding dynamic responses in different chaotic states by relying on Lyapunov exponent diagrams and bifurcation diagrams. Fang et al. [22] studied the discharge patterns in the three-dimensional memristive Izhikevich neuron model and constructed an MIZH neuronal network. It was found that it could show rich collective dynamical behaviors, and MIZH neuronal networks may remember and retrieve information efficiently. These investigations revealed that neuronal networks can exhibit several types of complex phenomena, including symmetry-breaking and period-doubling scenarios. It is well known that the nervous system has a large number of neurons with different biological structures and functions [23]. Therefore, it is necessary to develop more different memristive neuron and neural network models based on the different biological neuronal systems as well as different mathematical models.

As we know, energy is consumed so that neurons can save normal and continuous electric activity during the metabolic process of the neuronal system. Thus, it is interesting to detect the energy transmission and release dependencies on the electric activity mode in these neuronal models. In other words, the supply and consumption of energy is a key step in the metabolism and life activities of organisms. There also exists energy absorption and release in neurons and neural networks; the work of the brain is supported by energy [24–27]. In [28], the authors used Helmholtz's theorem to derive the Hamilton energy function of the dynamics system, which provided a theoretical basis for the calculation of energy. Lu et al. [29] estimated the dynamical behaviors and Hamilton energy of the improved memristive Hindmarsh–Rose neuron model under the effect of an external stimulation current and magnetic field. In their numerical simulations, the results showed that the transition of neuronal discharge patterns is closely related to energy changes, and the electrical activity patterns stimulated by periodic signals are more complex than those stimulated by mixed signals. Yang et al. [30] investigated the effect of periodic current and high–low-frequency electromagnetic radiation on neuronal discharge activity and energy; the model was built by a single Izhikevich neuron model under electromagnetic induction. The results revealed that the injection of stimulus signals can bring energy which is able to make the discharge mode transform to bursting. Besides the above-mentioned studies, there are many studies on the rich dynamic behavior of neuron models. However, the Hamilton energy of coupled neurons has rarely been reported in previous investigations;

the study of the interaction between coupled neurons is also a key step in exploring the mysteries of the brain.

Inspired by the above contributions, in the present paper, we will investigate the complex dynamical behavior and Hamilton energy of the coupled neuron model. The five-dimensional neuronal system with memristor synapses is presented in Section 2. The global exponential synchronization of the neuron system is proved in Section 3. Moreover, the Hamilton energy functions of the improved Izhikevich neuron system and the error system are derived by Helmholtz's theorem. In Section 4, numerical simulations are discussed, which describes the effects of the external stimulus current and parameters on the complex dynamics and energy in the improved system. Finally, Section 5 concludes the paper.

2. Model Description

To further understand how the brain works, we need to combine experimental studies of human nervous systems with the numerical simulation of large-scale brain models. A neuron model with a simple structure called the Izhikevich model was proposed in 2003, which has rich physiological meanings and unfolds all the known neural behaviors of the cortical neuron [31]. This model is suitable for large-scale simulations. Depending on four parameters, the model reproduces the spiking and bursting behavior of known types of cortical neurons.

The expression of the Izhikevich model is most consistent with the behavior of cortical neurons. The mathematical expression of this model can be described as follows:

$$\begin{cases} \frac{dv}{dt} = 0.04v^2 + 5v + 140 - u + I, \\ \frac{du}{dt} = a(bv - u). \end{cases} \tag{1}$$

with the post-spike resetting

$$\text{if } v \geq 30 \text{ mV,then} \begin{cases} c \to v, \\ u + d \to u. \end{cases}$$

where t is time, the variables v and u are the membrane potential and recovery variable in the Izhikevich neuron model (1), and I is the applied current. The control parameter a represents the rate of change in recovery variable u, and b represents the sensitivity of recovery variable u to the fluctuation of membrane potential v near the threshold. c, d represent the reset value of membrane potential v and recovery variable u after neuron discharges, which accounts for the activation of K^+ ionic currents and the inactivation of ${N_a}^+$ ionic currents, and it provides negative feedback to v. After the spike reaches its apex (+30 mV), the membrane voltage and the recovery variable are reset. Synaptic currents or injected dc currents are delivered via variable I. The $0.04v^2 + 5v + 140$ part was obtained by fitting the spike initiation dynamics of a cortical neuron so that the membrane potential v has an mV scale and the time has a scale. The resting potential in the model is between -70 and -60 mV depending on the value of b. Depending on the history of the membrane potential prior to the spike, the threshold potential can be as low as -55 mV or as high as -40 mV. By adjusting the value of these four parameters, the model can simulate spiking or bursting behaviors of neurons.

In the following, considering the existence of electromagnetic induction, a five-dimension neuron system is proposed by coupling two Izhikevich neurons with memristor synapses. The improved Izhikevich model can be written as follows:

$$\begin{cases} \frac{dv_1}{dt} = 0.04v_1^2 + 5v_1 + 140 - u_1 + I - k_1\rho(\varphi)(v_1 - v_2), \\ \frac{du_1}{dt} = a(bv_1 - u_1), \\ \frac{dv_2}{dt} = 0.04v_2^2 + 5v_2 + 140 - u_2 + I - k_1\rho(\varphi)(v_2 - v_1), \\ \frac{du_2}{dt} = a(bv_2 - u_2), \\ \frac{d\varphi}{dt} = k_2(v_1 - v_2) - k_3\varphi. \end{cases} \tag{2}$$

with the post-spike resetting

$$\text{if } v_i \geq 30 \text{ mV, then } \begin{cases} v \leftarrow c, \\ u \leftarrow u + d, \end{cases}$$

where v_i and u_i $(i = 1, 2)$ indicate membrane potentials and recovery variables in the coupled Izhikevich neuron model and φ describes the magnetic flux. $k_1\rho(\varphi)(v_1 - v_2)$ and $k_1\rho(\varphi)(v_2 - v_1)$ are the induced currents generated by electromagnetic induction in bidirectionally coupled neurons; $\rho(\varphi) = \alpha + 3\beta\varphi^2$ indicates memory conductance controlled by a magnetic flux in the memristor [32]; k_1 denotes the intensity of modulation of v_i by induced current; α is constant conductance; β is the feedback rate of magnetic flux; $k_2(v_1 - v_2)$ is the effect induced by v_i on magnetic flux; k_2 means the gain of the electromagnetic induction; $k_3\varphi$ is the magnetic leakage; k_3 means the flux feedback coefficient modulated by the neuron itself.

Analysis of Synchronous Stability

In this section, the global exponential synchronization of the corresponding model is proved by the Lyapunov stability theorem. In order to achieve the global exponential stability for the error system, the drive-response synchronization approach will be employed.

The drive system of the improved Izhikevich model is

$$\begin{cases} \frac{dv_1^{(1)}}{dt} = 0.04v_1^{(1)2} + 5v_1^{(1)} + 140 - u_1^{(1)} + I - k_1\rho(\varphi^{(1)})(v_1^{(1)} - v_2^{(1)}), \\ \frac{du_1^{(1)}}{dt} = a(bv_1^{(1)} - u_1^{(1)}), \\ \frac{dv_2^{(1)}}{dt} = 0.04v_2^{(1)2} + 5v_2^{(1)} + 140 - u_2^{(1)} + I - k_1\rho(\varphi^{(1)})(v_2^{(1)} - v_1^{(1)}), \\ \frac{du_2^{(1)}}{dt} = a(bv_2^{(1)} - u_2^{(1)}), \\ \frac{d\varphi^{(1)}}{dt} = k_2(v_1^{(1)} - v_2^{(1)}) - k_3\varphi^{(1)}. \end{cases} \tag{3}$$

Then, the response system is described as follows:

$$\begin{cases} \frac{dv_1^{(2)}}{dt} = 0.04v_1^{(2)2} + 5v_1^{(2)} + 140 - u_1^{(2)} + I - k_1\rho(\varphi^{(2)})(v_1^{(2)} - v_2^{(2)}) - U_1, \\ \frac{du_1^{(2)}}{dt} = a(bv_1^{(2)} - u_1^{(2)}) - U_2, \\ \frac{dv_2^{(2)}}{dt} = 0.04v_2^{(2)2} + 5v_2^{(2)} + 140 - u_2^{(2)} + I - k_1\rho(\varphi^{(2)})(v_2^{(2)} - v_1^{(2)}) - U_3, \\ \frac{du_2^{(2)}}{dt} = a(bv_2^{(2)} - u_2^{(2)}) - U_4, \\ \frac{d\varphi^{(2)}}{dt} = k_2(v_1^{(2)} - v_2^{(2)}) - k_3\varphi^{(2)}. \end{cases} \tag{4}$$

In Equation (4), $U_i(i = 1, 2, 3, 4)$ is the controllers which are the nonlinear functions designed. Let $e_1 = v_1^{(2)} - v_1^{(1)}$, $e_2 = u_1^{(2)} - u_1^{(1)}$, $e_3 = v_2^{(2)} - v_2^{(1)}$, $e_4 = u_2^{(2)} - u_2^{(1)}$, $e_5 = \varphi^{(2)} - \varphi^{(1)}$, so the error system of the drive system and the response system can be calculated. The synchronization manifold is as follows:

$$\begin{cases} \frac{de_1}{dt} & = 0.04(v_1^{(2)} + v_1^{(1)})e_1 + 5e_1 - e_2 - k_1\alpha e_1 + k_1\alpha e_3 \\ & -3k_1\beta[(\varphi^{(2)2}v_1^{(2)} - \varphi^{(1)2}v_1^{(1)}) - (\varphi^{(2)2}v_2^{(2)} - \varphi^{(1)2}v_2^{(1)})] + U_1, \\ \frac{de_2}{dt} & = abe_1 - ae_2 + U_2, \\ \frac{de_3}{dt} & = 0.04(v_2^{(2)} + v_2^{(1)})e_3 + 5e_3 - e_4 - k_1\alpha e_3 + k_1\alpha e_1 \\ & -3k_1\beta[(\varphi^{(2)2}v_2^{(2)} - \varphi^{(1)2}v_2^{(1)}) - (\varphi^{(2)2}v_1^{(2)} - \varphi^{(1)2}v_1^{(1)})] + U_3, \\ \frac{de_4}{dt} & = abe_3 - ae_4 + U_4, \\ \frac{de_5}{dt} & = k_2(e_1 - e_3) - k_3e_5. \end{cases} \tag{5}$$

Theorem 1. *The given initial value of the drive system (3) is* $(v_1^{(1)}(t_0), u_1^{(1)}(t_0), v_2^{(1)}(t_0), u_2^{(1)}(t_0), \varphi^{(1)}(t_0))$, *and the initial value of the response system (4) is taken as* $(v_1^{(2)}(t_0), u_1^{(2)}(t_0), v_2^{(2)}(t_0), u_2^{(2)}(t_0), \varphi^{(2)}(t_0))$.

The controllers are designed as follows:

$$\begin{cases} U_1 = & -0.04(v_1^{(2)} + v_1^{(1)})e_1 + k_1\alpha e_1 + 3k_1\beta[(\varphi^{(2)2}v_1^{(2)} - \varphi^{(1)2}v_1^{(1)}) \\ & -(\varphi^{(2)2}v_2^{(2)} - \varphi^{(1)2}v_2^{(1)})] - k_1\alpha e_3 - k_2e_5 - 6e_1^2, \\ U_2 = & -abe_1 + e_1, \\ U_3 = & -0.04(v_2^{(2)} + v_2^{(1)})e_3 + k_1\alpha e_3 + 3k_1\beta[(\varphi^{(2)2}v_2^{(2)} - \varphi^{(1)2}v_2^{(1)}) \\ & -(\varphi^{(2)2}v_1^{(2)} - \varphi^{(1)2}v_1^{(1)})] + k_1\alpha e_3 + k_2e_5 - 6e_3^2, \\ U_4 = & -abe_3 + e_3. \end{cases}$$

Here, $a > 0$, $k_3 > 0$, and the zero solution of the error system (5) satisfies the following inequality: $e_1^2(t) + e_2^2(t) + e_3^2(t) + e_4^2(t) + e_5^2(t) \leq k(\|e(t_0)\|)e^{-\alpha(t-t_0)}$; here, $k(\|e(t_0)\|)$ is a constant which depends on $\|e(t_0)\|$, and then, the zero solution of the error system (5) is globally exponentially stable, and the drive system (3) and the response system (4) can be realized as the global exponential synchronization.

Proof. According to the description of the controllers $U_i(i = 1, 2, 3, 4)$, Equation (5) can be rewritten in the following format:

$$\begin{cases} \frac{de_1}{dt} = -e_1 - e_2 - k_2e_5, \\ \frac{de_2}{dt} = e_1 - ae_2, \\ \frac{de_3}{dt} = -e_3 - e_4 + k_2e_5, \\ \frac{de_4}{dt} = e_3 - ae_4, \\ \frac{de_5}{dt} = k_2e_1 - k_2e_3 - k_3e_5. \end{cases} \tag{6}$$

We construct the Lyapunov function as follows:

$$V = \frac{1}{2}(e_1^2 + e_2^2 + e_3^2 + e_4^2 + e_5^2) = (e_1, e_2, e_3, e_4, e_5)P(e_1, e_2, e_3, e_4, e_5)^T$$

Suppose that $\lambda_{\min}(P)$ is the smallest eigenvalue of the matrix P, $\lambda_{\max}(P)$ is the largest eigenvalue of the matrix P, and $P = diag(\frac{1}{2}, \frac{1}{2}, \frac{1}{2}, \frac{1}{2}, \frac{1}{2})$; thus,

$$\begin{aligned}
\tfrac{dV}{dt} &= \dot{e}_1 e_1 + \dot{e}_2 e_2 + \dot{e}_3 e_3 + \dot{e}_4 e_4 + \dot{e}_5 e_5, \\
&= (-e_1 - e_2 - k_2 e_5) e_1 + (e_1 - a e_2) e_2 + (-e_3 - e_4 + k_2 e_5) e_3 + (e_3 - a e_4) e_4 \\
&+ (k_2 e_1 - k_2 e_3 - k_3 e_5) e_5, \\
&= -e_1^2 - a e_2^2 - e_3^2 - a e_4^2 - k_3 e_5^2, \\
&\leq -|e_1|^2 - a|e_2|^2 - |e_3|^2 - a|e_4|^2 - k_3|e_5|^2, \\
&\leq (|e_1|, |e_2|, |e_3|, |e_4|, |e_5|) A (|e_1|, |e_2|, |e_3|, |e_4|, |e_5|)^T.
\end{aligned} \tag{7}$$

where

$$A = \begin{pmatrix} -1 & 0 & 0 & 0 & 0 \\ 0 & -a & 0 & 0 & 0 \\ 0 & 0 & -1 & 0 & 0 \\ 0 & 0 & 0 & -a & 0 \\ 0 & 0 & 0 & 0 & -k_3 \end{pmatrix}.$$

Assume that $\lambda_{\max}(A)$ is the largest eigenvalue of matrix A, since $A < 0$; then, $\lambda_{\max}(A) < 0$.

$$\begin{aligned}
\tfrac{dV}{dt} &\leq \lambda_{\max}(A)(e_1^2 + e_2^2 + e_3^2 + e_4^2 + e_5^2) \\
&\leq \lambda_{\max}(A) \tfrac{\lambda_{\max}(P)}{\lambda_{\max}(P)} (e_1^2 + e_2^2 + e_3^2 + e_4^2 + e_5^2) \\
&\leq \tfrac{\lambda_{\max}(A)}{\lambda_{\max}(P)} [\lambda_{\max}(P)(e_1^2 + e_2^2 + e_3^2 + e_4^2 + e_5^2)] \\
&\leq \tfrac{\lambda_{\max}(A)}{\lambda_{\max}(P)} V.
\end{aligned} \tag{8}$$

$$V(x(t)) \leq V(x(t_0)) e^{\frac{\lambda_{\max}(A)}{\lambda_{\max}(P)}(t - t_0)}. \tag{9}$$

Hence,

$$\lambda_{\min}(P)(e_1^2 + e_2^2 + e_3^2 + e_4^2 + e_5^2) \leq V(x(t)), \tag{10}$$

$$e_1^2 + e_2^2 + e_3^2 + e_4^2 + e_5^2 \leq \frac{V(x(t))}{\lambda_{\min}(P)} \leq \frac{V(x(t_0))}{\lambda_{\min}(P)} e^{\frac{\lambda_{\max}(A)}{\lambda_{\max}(P)}(t - t_0)}, \tag{11}$$

Here, $x(t) = (e_1(t), e_2(t), e_3(t), e_4(t), e_5(t))$, $x(t_0) = (e_1(t_0), e_2(t_0), e_3(t_0), e_4(t_0), e_5(t_0))$.

Therefore, the zero solution of the error system (5) is globally exponentially stable, and the drive system (3) and the response system (4) achieve global exponential synchronization. □

3. Hamilton Energy of the Izhikevich Model

A neuron under an electromagnetic environment is accompanied by the conversion and migration of energy. And the support of energy in the brain is essential for the discharge activity of a neuron. Here, the Hamilton energy functions are determined, which are associated with the coupled Izhikevich neuron model and the corresponding error system. Based on Helmholtz's theorem [33], the Hamilton energy function of the neuron model could be calculated. Helmholtz's theorem decomposes an arbitrary electromagnetic field $F(x)$ into the superposition of a gradient field $f_d(x)$ and a vortex field $f_c(x)$, and its dynamical equation can be expressed by Equation (12).

$$F(x) = f_c(x) + f_d(x) = [J(x) + R(x)] \nabla H, \tag{12}$$

where $f_c(x)$ represents the conservative component and $f_d(x)$ represents the dissipative component, and $J(x)$ is a skew-symmetric matrix and $R(x)$ is a symmetric matrix. ∇H indicates the gradient matrix of the Hamilton energy function $H(x)$.

The Hamilton energy function must be satisfied as

$$\begin{cases} \dot{H} = \frac{dH}{dt} = \nabla H^T f_d(x), \\ \nabla H^T f_c(x) = 0. \end{cases} \tag{13}$$

Therefore, system (2) is rewritten as

$$\begin{pmatrix} \frac{dv_1}{dt} \\ \frac{du_1}{dt} \\ \frac{dv_2}{dt} \\ \frac{du_2}{dt} \\ \frac{d\varphi}{dt} \end{pmatrix} = f_c(v_1, u_1, v_2, u_2, \varphi) + f_d(v_1, u_1, v_2, u_2, \varphi), \tag{14}$$

with

$$f_c(v_1, u_1, v_2, u_2, \varphi) = J \cdot \nabla H = \begin{pmatrix} 140 - u_1 + I + k_1\rho(\varphi)v_2 - \varphi \\ abv_1 \\ 140 - u_2 + I + k_1\rho(\varphi)v_1 + \varphi \\ abv_2 \\ k_2(v_1 - v_2) \end{pmatrix}.$$

$$f_d(v_1, u_1, v_2, u_2, \varphi) = R \cdot \nabla H = \begin{pmatrix} 0.04v_1^2 + 5v_1 - k_1\rho(\varphi)v_1 + \varphi \\ -au_1 \\ 0.04v_2^2 + 5v_2 - k_1\rho(\varphi)v_2 - \varphi \\ -au_2 \\ -k_3\varphi \end{pmatrix}.$$

By combining Equation (13) with Equation (14), one can obtain

$$\begin{aligned} &(140 - u_1 + I + k_1\rho(\varphi)v_2 - \varphi)\tfrac{\partial H}{\partial v_1} + (abv_1)\tfrac{\partial H}{\partial u_1} \\ &+(140 - u_2 + I + k_1\rho(\varphi)v_1 - \varphi)\tfrac{\partial H}{\partial v_2} + (abv_2)\tfrac{\partial H}{\partial u_2} + k_2(v_1 - v_2)\tfrac{\partial H}{\partial \varphi} = 0. \end{aligned} \tag{15}$$

The general solution of Equation (15) is expressed as

$$\begin{aligned} H &= (140 - u_1 + I + k_1\rho(\varphi)v_2 - \varphi)^2 + abv_1^2 \\ &+(140 - u_2 + I + k_1\rho(\varphi)v_1 + \varphi)^2 + abv_2^2 + k_2(v_1 - v_2)^2. \end{aligned} \tag{16}$$

The derivative of the Hamilton energy function versus time is denoted by

$$\begin{aligned} \tfrac{dH}{dt} &= 2(140 - u_1 + I + k_1\rho(\varphi)v_2 - \varphi)(-\dot{u}_1 + k_1\rho(\varphi)\dot{v}_2 - \dot{\varphi}) + 2abv_1\dot{v}_1 \\ &+2(140 - u_2 + I + k_1\rho(\varphi)v_1 + \varphi)(-\dot{u}_2 + k_1\rho(\varphi)\dot{v}_1 + \dot{\varphi}) + 2abv_2\dot{v}_2 \\ &+2ab(v_1 - v_2)(\dot{v}_1 - \dot{v}_2). \end{aligned} \tag{17}$$

Substituting the values of system (2), we find that

$$\begin{aligned} \tfrac{dH}{dt} &= [0.04v_1^2 + 5v_1 - k_1\rho(\varphi)v_1 + \varphi][(140 - u_2 + I + k_1\rho(\varphi)v_1 + \varphi)] \\ &+2abv_1 + 2k_1\rho(\varphi)[2k_2(v_1 - v_2)] + (-au_1)[-2(140 - u_1 + I + k_1\rho(\varphi)v_2 - \varphi)] \\ &+[0.04v_2^2 + 5v_2 - k_1\rho(\varphi)v_2 - \varphi][2abv_2 + 2k_1\rho(\varphi)(140 - u_1 + I + k_1\rho(\varphi)v_2 - \varphi)] \\ &+[2abv_2 + 2k_1\rho(\varphi)][2k_2(v_1 - v_2)](-au_2)[-2(140 - u_2 + I + k_1\rho(\varphi)v_1 - \varphi)] \\ &+(-k_3\varphi)[-2(140 - u_1 + I + k_1\rho(\varphi)v_2 - \varphi) + 2(140 - u_2 + I + k_1\rho(\varphi)v_1 + \varphi)]. \end{aligned} \tag{18}$$

In addition,

$$\frac{dH}{dt} = \nabla H^T f_d(x) = [\alpha_1\ \alpha_2\ \alpha_3\ \alpha_4\ \alpha_5] \begin{bmatrix} 0.04v_1^2 + 5v_1 - k_1\rho(\varphi)v_1 + \varphi \\ -au_1 \\ 0.04v_2^2 + 5v_2 - k_1\rho(\varphi)v_2 - \varphi \\ -au_2 \\ -k_3\varphi \end{bmatrix}, \tag{19}$$

with

$$\begin{aligned}
\alpha_1 &= 2abv_1 + 2k_1\rho(\varphi)(140 - u_2 + I + k_1\rho(\varphi)v_1 + \varphi) + 2k_2(v_1 - v_2),\\
\alpha_2 &= -2(140 - u_1 + I + k_1\rho(\varphi)v_2 - \varphi),\\
\alpha_3 &= 2abv_2 + 2k_1\rho(\varphi)(140 - u_1 + I + k_1\rho(\varphi)v_2 - \varphi) + 2k_2(v_1 - v_2),\\
\alpha_4 &= -2(140 - u_2 + I + k_1\rho(\varphi)v_1 - \varphi),\\
\alpha_5 &= -2(140 - u_1 + I + k_1\rho(\varphi)v_2 - \varphi) + 2(140 - u_2 + I + k_1\rho(\varphi)v_1 + \varphi).
\end{aligned}$$

According to the above derivation, H satisfies the existence condition of the Hamilton energy function in Equation (13), and Equation (16) is the Hamilton energy function requested.

Next, we derive the Hamilton energy function H' of the error system (6) to study the flow of energy in the maintenance of synchronization. According to the above theorem, we rewrite system (6) as follows:

$$\begin{pmatrix} \frac{de_1}{dt} \\ \frac{de_2}{dt} \\ \frac{de_3}{dt} \\ \frac{de_4}{dt} \\ \frac{de_5}{dt} \end{pmatrix} = f_c'(e_1, e_2, e_3, e_4, e_5) + f_d'(e_1, e_2, e_3, e_4, e_5), \tag{20}$$

with

$$f_c'(e_1, e_2, e_3, e_4, e_5) = J \cdot \nabla H' = \begin{pmatrix} -e_2 - k_2e_5 \\ e_1 \\ -e_4 + k_2e_5 \\ e_3 \\ k_2e_1 - k_2e_3 \end{pmatrix}, f_d'(e_1, e_2, e_3, e_4, e_5) = R \cdot \nabla H' = \begin{pmatrix} -e_1 \\ -ae_2 \\ -e_3 \\ -ae_4 \\ -k_3e_5 \end{pmatrix}.$$

Then, we obtain

$$(-e_2 - k_2e_5)\frac{\partial H'}{\partial e_1} + (e_1)\frac{\partial H'}{\partial e_2} + (-e_4 + k_2e_5)\frac{\partial H'}{\partial e_3} + (e_3)\frac{\partial H'}{\partial e_4} + (k_2e_1 - k_2e_3)\frac{\partial H'}{\partial e_5} = 0, \tag{21}$$

the general solution of Equation (21) is expressed as

$$H' = (-e_2 - k_2e_5)^2 + e_1^2 + (-e_4 + k_2e_5)^2 + e_3^2 + (k_2e_1 - k_2e_3)^2, \tag{22}$$

the derivative of the Hamilton energy function versus time is denoted by

$$\begin{aligned}
\tfrac{dH'}{dt} \quad &= 2(-e_2 - k_2e_5)(-\dot{e}_2 - k_2\dot{e}_5) + 2e_1\dot{e}_1\\
&+2(-e_4 + k_2e_5)(-\dot{e}_4 + k_2\dot{e}_5) + 2e_3\dot{e}_3 + 2(k_2e_1 - k_2e_3)(k_2\dot{e}_1 - k_2\dot{e}_3).
\end{aligned} \tag{23}$$

Substituting the values of system (6), we can obtain

$$\begin{aligned}\frac{dH'}{dt} &= [2e_1 + 2k_2(k_2e_1 - k_2e_3)](-e_1) - 2(-e_2 - k_2e_5)(-ae_2)\\ &+[2e_3 - 2k_2(k_2e_1 - k_2e_3)](-e_3) - 2(-e_{34} + k_2e_5)(-ae_4)\\ &+[-2k_2(e_2 - k_2e_5) + 2k_2(-e_4 + k_2e_5)](-k_3e_5).\end{aligned} \tag{24}$$

Therefore, Equation (22) is the Hamilton energy function of the error system.

4. Numerical Simulations

In this section, to better understand the dynamical behavior of the improved Izhikevich neuron system, numerical simulations are performed under different values of the parameters. Here, we use MATLAB software to plot all the figures. The integration is performed using the fourth-order Runge–Kutta algorithm with a time step of $h = 10^{-3}$.

The parameters are taken as $I = 2$, $k_1 = 0.2$, $k_2 = 0.53$, $k_3 = 0.32$, $\alpha = 0.4$, and $\beta = 0.02$. In addition, the values of the parameters related to the excitatory neuron and the inhibitory neuron are selected as $a = 0.02$, $b = 0.2$, $c = -50$, and $d = 2$ and $a = 0.1$, $b = 0.2$, $c = -65$, and $d = 2$, respectively. Figure 1 shows the phase portrait of the improved Izhikevich neuron system (2); system (2) exhibits dynamics from stability to chaos. Chaos occurs when the value of membrane potential is larger than 30 mV, which is due to the auxiliary after-spike resetting of the Izhikevich neuron model.

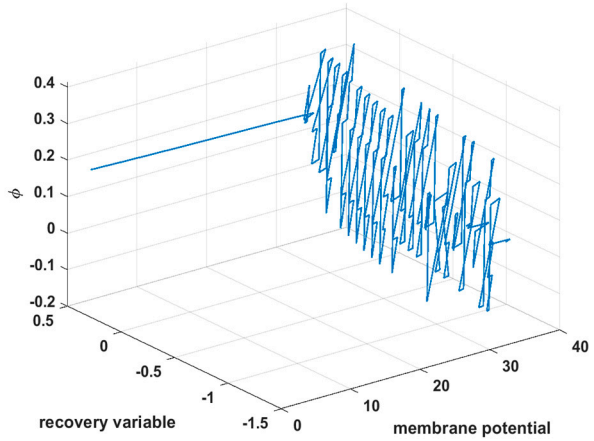

Figure 1. Phase portrait of the improved Izhikevich neuron system (2).

The variations in discharge patterns in the excitatory and inhibitory neurons are explored by setting three groups' initial values in the improved Izhikevich neuron system (2). The time series of membrane potential with different initial conditions are plotted in Figure 2. It is shown that the discharge patterns exhibit chattering peaks if the coupled neurons are all excited, and the internal chattering frequency and the time interval of chattering are different within the three groups of initial values in Figure 2a. And the discharge patterns of the neuron appear as inhibition spiking if the coupled neurons are all inhibited. It is shown that the frequencies of spiking peaks become higher in comparison with the excitatory neuron in Figure 2b. As a consequence, changing the initial conditions can produce different discharge modes in the different types of neurons in system (2).

As shown in Figure 3, the time series of the membrane potential are plotted by applying an external stimulus current at amplitude fixation or frequency fixation within the coupled neurons in system (2). At amplitude fixation, the neurons exist in a refractory period which is affected by the frequency of the stimulation current. The coupled excitatory neuronal system presents the chattering pattern, and the chattering frequency is the inequality in Figure 3a. When the frequency is fixed, the refractory period of neurons disappears gradually. The time series of the membrane potential transform from an inhibition bursting to a tonic bursting action sequence, the time interval between chattering peaks decreases,

and the discharge mode becomes more regular, as shown in Figure 3b. It is found that the frequency of the external stimulation current has little effect on inhibitory neurons, as shown in Figure 3c. As depicted in Figure 3d, the discharge mode transforms from spiking to inhibition bursting, and the frequency of the discharge spike increases. Thereby, it is concluded that the discharge mode of the neuron system changes with the amplitude and frequency of the external stimulus current.

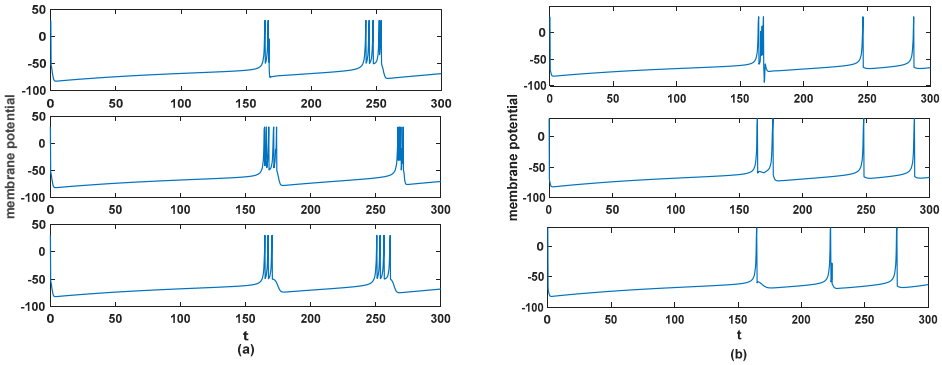

Figure 2. Time series of the membrane potential under different initial conditions in system (2); system parameters are taken as $I = 2$, $k_1 = 0.2$, $k_2 = 0.53$, $k_3 = 0.32$. (**a**) The excited neurons when the initial values are selected as $(0.25, 0.3, 0.35, 0.13, 0.2)$. (**b**) The inhibited neurons when the initial values are taken as $(0.25, 0, 0.25, 0, 0.2)$. When the external current is applied to the neuronal system, the discharge modes of the system could be accompanied by the variation in energy. The performance of discharge activities and Hamilton energy are investigated by applying external stimulus current $I = A\cos(Bt)$ under the coupled excitatory or inhibitory neurons in system (2).

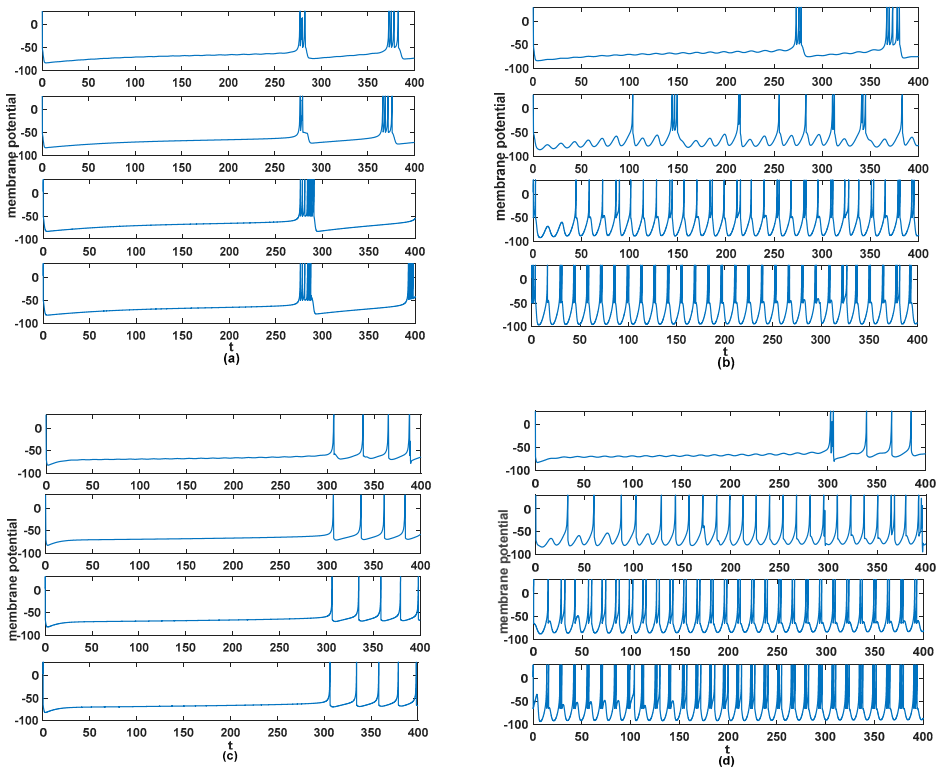

Figure 3. Time series of the membrane potential by applying external stimulus current $I = A\cos(Bt)$ in system (2). (**a**) Time series of excitatory neurons with $A = 0.2$ and $B = 0.5, 5, 15, 25$. (**b**) Time series of excitatory neurons with $B = 0.45$ and $A = 0.7, 7, 17, 27$. (**c**) Time series of inhibitory neurons with $A = 0.2$ and $B = 0.5, 5, 15, 25$. (**d**) Time series of inhibitory neurons with $B = 0.45$ and $A = 0.7, 7, 17, 27$.

In order to further investigate the overall influence of amplitude A and frequency B on the discharge activity and energy of the excitatory neuron in system (2), the bifurcation diagram (ISI) and the largest Lyapunov exponent diagram (LLE) are plotted in Figure 4. The effect of the frequency and amplitude of the external stimulus current on the dynamics behavior of neurons is consistent in terms of excitability and inhibitability. From Figure 4a,b, it can be observed that the neuron model shifts from chaos to stability, and its corresponding largest Lyapunov exponent turns from greater than zero to equal to zero. That is, the coupled neuron system transforms from chaotic to periodic as the amplitude increases. And as can be seen from Figure 4b,d, chaotic and periodic behaviors coexist in the coupled neuron system as the frequency increases. Therefore, the amplitude of external current stimulation can promote periodic discharge activity of the neuron model.

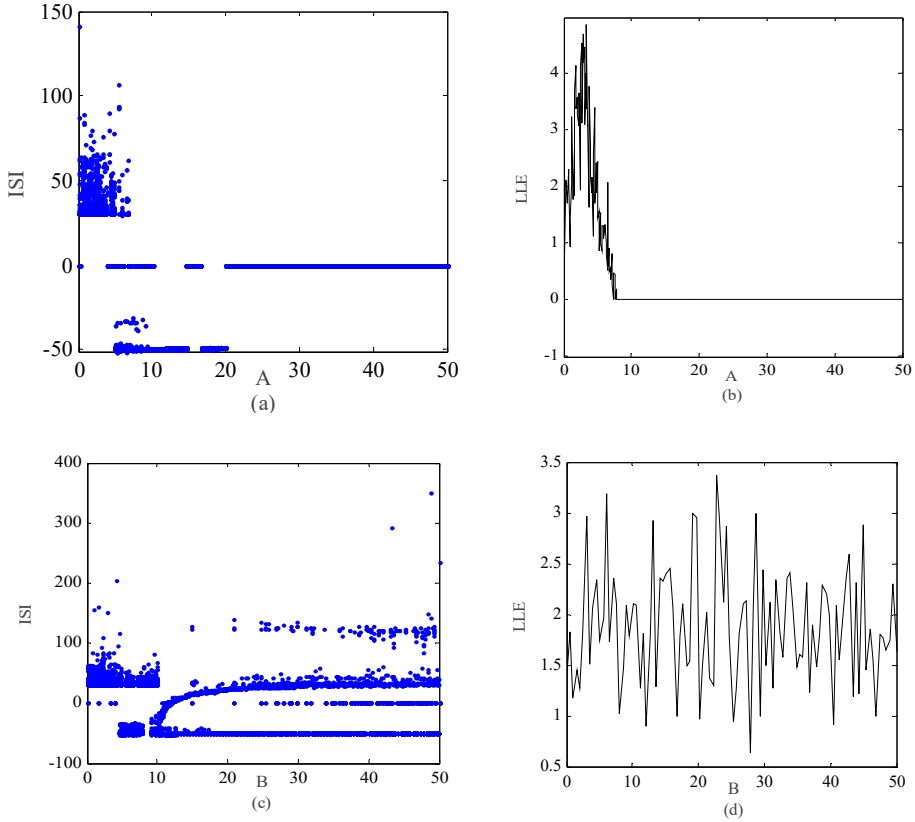

Figure 4. Dynamical behaviors of system (2) with different values for the amplitude A and frequency B of the external stimulus current. (**a**) Bifurcation diagram of the related parameters with amplitude A for $B = 0.45$. (**b**) The largest Lyapunov exponent-related parameters with the amplitude A for $B = 0.45$. (**c**) Bifurcation diagram of the related parameters with frequency B for $A = 0.2$. (**d**) The largest Lyapunov exponent related parameters with frequency B for $A = 0.2$.

In Figure 5, the amplitude A and frequency B are chosen as variables to characterize the transformation of the energy in system (2). The evolution of energy is consistent with the dynamical behavior of system (2). It is shown that the Hamilton energy with respect to the dynamical behavior decreases as the amplitude A increases, which corresponds exactly to the amplitude control of the system in Figure 5a. And the energy shows a smooth change as frequency B increases in Figure 5b. The two-parameter figures of the Hamilton energy of system (2) are plotted in Figure 5c,d; the energy varies with a periodic state when the amplitude A and frequency B are varied simultaneously. These results demonstrate that the energy of system (2) depends on the transformation of amplitude A or frequency B, and the energy requirement for the chaotic discharge activities is more than the other one for the periodic discharge activities in the neuronal system.

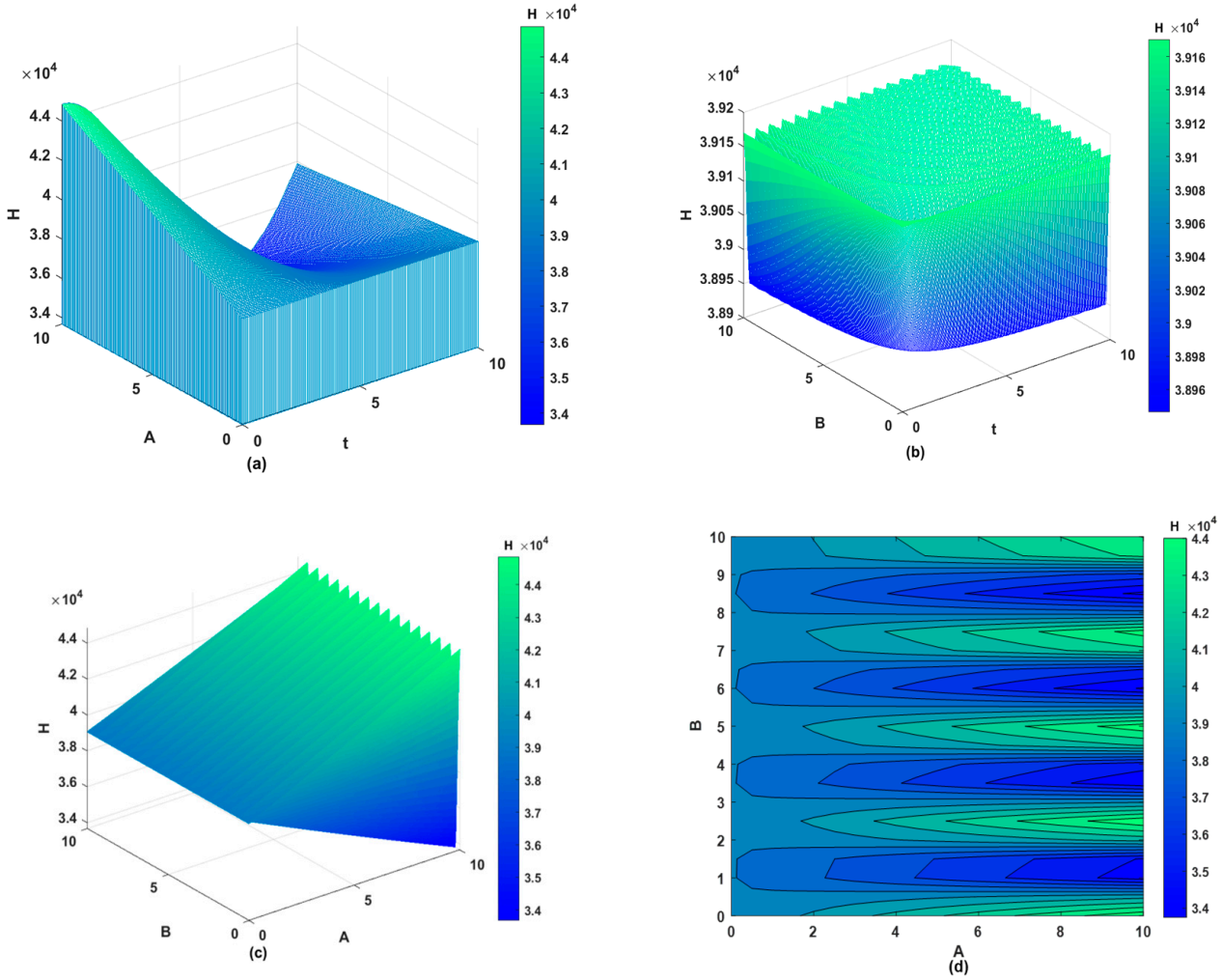

Figure 5. Evolutions of the Hamilton energy function related with different values of external stimulus current within the coupled neurons in system (2). (**a**) The evolution of Hamilton energy with respect to the amplitude A. (**b**) The evolution of Hamilton energy with respect to the frequency B. (**c**) The evolution of Hamilton energy with the amplitude A and frequency B. (**d**) Planar graphics based on the three-dimensional figure (**c**).

On the other hand, it is noticed that the modulation intensity of the induced current k_1 and the gain in the electromagnetic induction k_2 play important roles in the expression of Hamilton energy function. The following Figure 6a–d show the complex dynamical behavior of the coupled neurons with the changing parameters k_1 and k_2. When the coupled neurons are all excited, the coupled neurons present a mixture of periodic and chaotic states. Nevertheless, when the coupled neurons are all inhibited, system (2) transforms from periodic to chaotic as k_1 increases, and it maintains multi-periodicity all the time as k_2 increases, as shown in Figure 6c,d. Moreover, the evolutions of the Hamilton energy function related to k_1 and k_2 are depicted in Figure 7. We find that the Hamilton energy of system (2) increases as k_1 changes, whereas parameter k_2 does not cause the energy to change. Compared to Figures 6 and 7, the results imply that the gain in the electromagnetic induction can modulate the energy released by the neuron model.

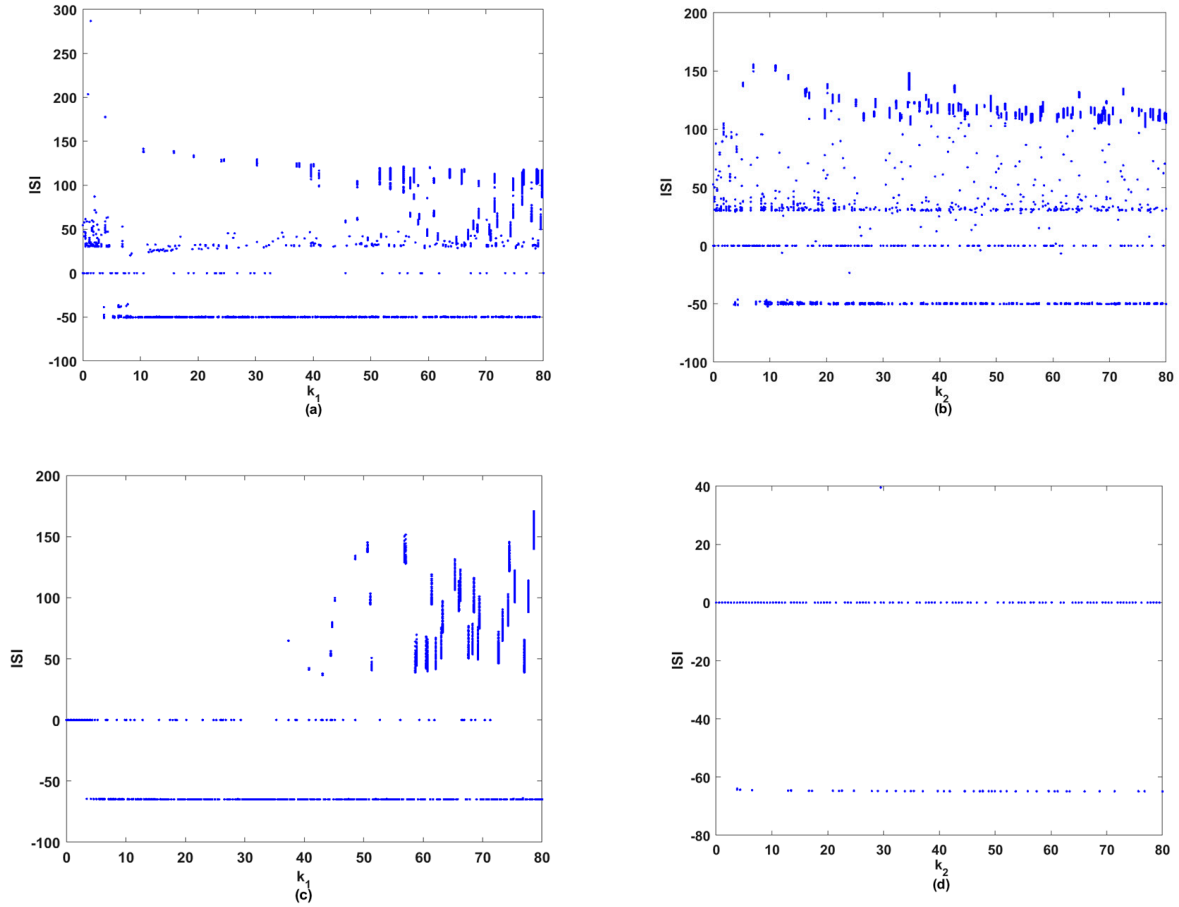

Figure 6. Bifurcation diagrams related to k_1 and k_2 in system (2); the initial values and parameters are selected as $(0.25,\ 0.3,\ 0.35,\ 0.13,\ 0.2)$, $I = 5$, $k_3 = 0.32$. (**a**) Bifurcation diagram of the excitatory neurons for $k_2 = 0.53$. (**b**) Bifurcation diagram of the inhibitory neurons for $k_1 = 0.2$. (**c**) Bifurcation diagram of the inhibitory neurons for $k_2 = 0.53$. (**d**) Bifurcation diagram of the excitatory neurons for $k_1 = 0.2$.

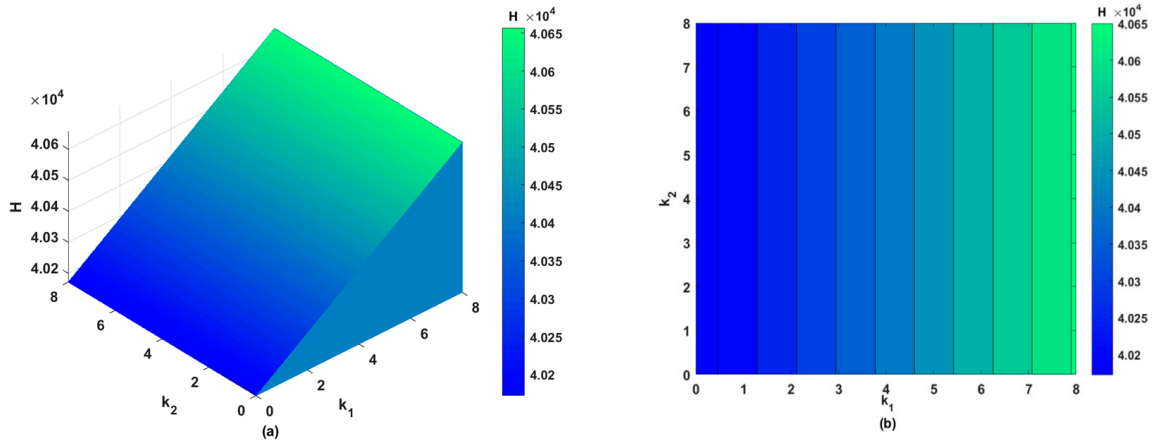

Figure 7. Evolutions of the Hamilton energy function related with k_1 or k_2 within coupled neurons in system (2). The parameters are taken as $(0.25,\ 0.3,\ 0.35,\ 0.13,\ 0.2)$, $I = 5$, $k_3 = 0.32$, for (**a**) $k_2 = 0.53$ and (**b**) $k_1 = 0.2$.

5. Conclusions

In summary, the dynamical behavior of the coupled Izhikevich neuron model using the memristor synapse has been investigated. Based on the Lyapunov stability theorem,

the condition of the global exponential synchronization of the improved Izhikevich neuron model has been derived. Meanwhile, we analyzed the Hamilton energy functions associated with the improved Izhikevich neuron model and its error system according to Helmholtz's theorem.

Furthermore, the influence of the parameters of the external stimulus currents and the electromagnetic induction has been investigated. Numerical computations indicated that the amplitude of external current stimulation can promote periodic discharge activity of the neuron model. In addition, the amount of energy for the chaotic state could be more than that for the periodic state during the discharge activity in the neuronal system. The dynamical behavior of the neuron model transforms from periodic to chaotic as the modulation intensity of the induced current increases, while the gain in the electromagnetic induction can maintain the periodic discharge pattern and modulate the energy released by the neuron model.

Our approach can be extended to investigate the energy aspects of different oscillatory regimes of nonidentical oscillators. The theorem results will be useful to study the energy aspects of other coupled complex systems. Possible extensions to neural networks can provide finer insight into the energy modulation mechanisms of various biological systems. Moreover, these results may help us better understand the relationship between electrical activity and energy and further understand the energy characteristics of complex systems under different dynamical behaviors.

Author Contributions: F.J.: writing—original draft, revisions, software; P.H.: revisions, analysis; L.Y.: supervision, writing—review and editing. All authors have read and agreed to the published version of the manuscript.

Funding: This work was partly supported by the NSF of China under Grant Nos. 11702195.

Data Availability Statement: The datasets generated and analyzed during the current study are available from the corresponding author upon reasonable request.

Conflicts of Interest: The authors declare no conflicts of interest.

References

1. Gerstner, W.; Naud, R. How good are neuron models? *Science* **2009**, *326*, 379–380. [CrossRef]
2. Hodgkin, A.L.; Huxley, A.F. Currents carried by sodium and potassium ions through the membrane of the giant axon of *Loligo*. *J. Physiol.* **1952**, *116*, 449–472. [CrossRef]
3. FitzHugh, R. Impulses and physiological states in theoretical models of nerve membrane. *Biophys. J.* **1961**, *1*, 445–466. [CrossRef]
4. Nagumo, J.; Arimoto, S.; Yoshizawa, S. An active pulse transmission line simulating nerve axon. *Proc. IRE* **1962**, *50*, 2061–2070. [CrossRef]
5. Chay, T.R. Chaos in a three-variable model of an excitable cell. *Physica D* **1985**, *16*, 233–242. [CrossRef]
6. Rose, R.M.; Hindmarsh, J.L. The assembly of ionic currents in a thalamic neuron I. The three-dimensional model. *Proc. R. Soc. Lond. B Biol. Sci.* **1989**, *237*, 267–288.
7. Hopfield, J.J. Hopfield network. *Scholarpedia* **2007**, *2*, 1977. [CrossRef]
8. Izhikevich, E.M. Simple model of spiking neurons. *IEEE Trans. Neural Netw.* **2003**, *14*, 1569–1572. [CrossRef]
9. Akopyan, F.; Sawada, J.; Cassidy, A.; Alvarez-Icaza, R.; Arthur, J.; Merolla, P.; Imam, N.; Nakamura, Y.; Datta, P.; Nam, G.J.; et al. Truenorth: Design and tool flow of a 65 mw 1 million neuron programmable neurosynaptic chip. *IEEE Trans. Comput.-Aided Des. Integr. Circuits Syst.* **2015**, *34*, 1537–1557. [CrossRef]
10. An, X.L.; Qiao, S. The hidden, period-adding, mixed-mode oscillations and control in a HR neuron under electromagnetic induction. *Chaos Solitons Fractals* **2021**, *143*, 110587. [CrossRef]
11. Menale, M.; Carbonaro, B. The mathematical analysis towards the dependence on the initial data for a discrete thermostatted kinetic framework for biological systems composed of interacting entities. *AIMS Biophys.* **2020**, *7*, 204–218. [CrossRef]
12. Shen, H.; Yu, F.; Kong, X.; Mokbel, A.A.M.; Wang, C.; Cai, S. Dynamics study on the effect of memristive autapse distribution on Hopfield neural network. *Chaos* **2022**, *32*, 083133. [CrossRef]
13. Tagne Nkounga, I.B.; Goulefack, L.M.; Yamapi, R.; Kurths, J. Switching from active to non-active states in a birhythmic conductance-based neuronal model under electromagnetic induction. *Nonlinear Dyn.* **2023**, *111*, 771–788. [CrossRef]
14. Lakshmanan, S.; Lim, C.P.; Nahavandi, S.; Prakash, M.; Balasubramaniam, P. Dynamical analysis of the Hindmarsh–Rose neuron with time delays. *IEEE Trans. Neural Netw. Learn. Syst.* **2016**, *28*, 1953–1958. [CrossRef]
15. Zhang, Y.; Wang, C.; Tang, J.; Ma, J.; Ren, G. Phase coupling synchronization of FHN neurons connected by a Josephson junction. *Sci. China Technol. Sci.* **2020**, *63*, 2328–2338. [CrossRef]

16. Lv, M.; Wang, C.; Ren, G. Model of electrical activity in a neuron under magnetic flow effect. *Nonlinear Dyn.* **2016**, *85*, 1479–1490. [CrossRef]
17. Ma, J.; Tang, J. A review for dynamics in neuron and neuronal network. *Nonlinear Dyn.* **2017**, *89*, 1569–1578. [CrossRef]
18. Karthikeyan, A.; Srinivasan, A.; Arun, S. Complex network dynamics of a memristor neuron model with piecewise linear activation function. *Eur. Phys. J. Spec. Top.* **2022**, *231*, 4089–4096. [CrossRef]
19. Xu, Q.; Liu, T.; Ding, S.; Bao, H.; Li, Z.; Chen, B. Extreme multistability and phase synchronization in a heterogeneous bi-neuron Rulkov network with memristive electromagnetic induction. *Cogn. Neurodyn.* **2023**, *17*, 755–766. [CrossRef]
20. Kafraj, M.S.; Parastesh, F.; Jafari, S. Firing patterns of an improved Izhikevich neuron model under the effect of electromagnetic induction and noise. *Chaos Solitons Fractals* **2020**, *137*, 109782. [CrossRef]
21. Mondal, A.; Mondal, A.; Sharma, S.K.; Upadhyay, R.K. Analysis of spatially extended excitable Izhikevich neuron model near instability. *Nonlinear Dyn.* **2021**, *105*, 3515–3527. [CrossRef]
22. Fang, X.; Duan, S.; Wang, L. Memristive Izhikevich Spiking Neuron Model and Its Application in Oscillatory Associative Memory. *Front. Neurosci.* **2022**, *16*, 885322. [CrossRef]
23. Gray, C.M.; McCormick, D.A. Chattering cells: Superficial pyramidal neurons contributing to the generation of synchronous oscillations in the visual cortex. *Science* **1996**, *274*, 109–113. [CrossRef]
24. Bellomo, N. *Modeling Complex Living Systems: A Kinetic Theory and Stochastic Game Approach*; Springer Science & Business Media: Berlin/Heidelberg, Germany, 2008.
25. Laughlin, S.B.; Sejnowski, T.J. Communication in neuronal networks. *Science* **2023**, *301*, 1870–1874. [CrossRef]
26. Njitacke, Z.T.; Awrejcewicz, J.; Ramakrishnan, B.; Rajagopal, K.; Kengne, J. Hamiltonian energy computation and complex behavior of a small heterogeneous network of three neurons: Circuit implementation. *Nonlinear Dyn.* **2022**, *107*, 2867–2886. [CrossRef]
27. Trigo, D.; Avelar, C.; Fernandes, M.; Sá, J.; da Cruz e Silva, O. Mitochondria, energy, and metabolism in neuronal health and disease. *FEBS Lett.* **2022**, *596*, 1095–1110. [CrossRef]
28. Chun-Ni, W.; Ya, W.; Jun, M. Calculation of Hamilton energy function of dynamical system by using Helmholtz theorem. *Acta Phys. Sin.* **2016**, *65*, 240501. [CrossRef]
29. Lu, L.; Jia, Y.; Xu, Y. Energy dependence on modes of electric activities of neuron driven by different external mixed signals under electromagnetic induction. *Sci. China Technol. Sci.* **2019**, *62*, 427–440. [CrossRef]
30. Yang, Y.; Ma, J.; Xu, Y.; Jia, Y. Energy dependence on discharge mode of Izhikevich neuron driven by external stimulus under electromagnetic induction. *Cogn. Neurodyn.* **2021**, *15*, 265–277. [CrossRef]
31. Xu, Y.; Jia, Y.; Kirunda, J.B.; Shen, J.; Ge, M.; Lu, L.; Pei, Q. Dynamic behaviors in coupled neuron system with the excitatory and inhibitory autapse under electromagnetic induction. *Complexity* **2018**, *2018*, 3012743. [CrossRef]
32. Chua, L. Memristor-the missing circuit element. *IEEE Trans. Circuit Theory* **1971**, *18*, 507–519. [CrossRef]
33. Song, X.L.; Jin, W.Y.; Ma, J. Energy dependence on the electric activities of a neuron. *Chin. Phys. B* **2015**, *24*, 128710. [CrossRef]

Disclaimer/Publisher's Note: The statements, opinions and data contained in all publications are solely those of the individual author(s) and contributor(s) and not of MDPI and/or the editor(s). MDPI and/or the editor(s) disclaim responsibility for any injury to people or property resulting from any ideas, methods, instructions or products referred to in the content.